Single-Stage Astaxanthin Production Enhances the Nonmevalonate Pathway and Photosynthetic Central Metabolism in Synechococcus sp. PCC 7002

Hasunuma, Tomohisa ; Takaki, Ayako ; Matsuda, Mami ; Kato, Yuichi ; Vavricka, Christopher J. ; Kondo, Akihiko

(Citation)
ACS synthetic biology,8(12):2701-2709

(Issue Date)
2019-10-25

(Resource Type)
journal article

(Version)
Accepted Manuscript

ACS Synthetic Biology

Article

Single-stage astaxanthin production enhances the non-mevalonate pathway and photosynthetic central metabolism in *Synechococcus* sp. PCC 7002

Tomohisa Hasunuma, Ayako Takaki, Mami Matsuda,
Yuichi Kato, Christopher J. Vavricka, and Akihiko Kondo

ACS Synth. Biol., **Just Accepted Manuscript** • DOI: 10.1021/acssynbio.9b00280 • Publication Date (Web): 25 Oct 2019

is published by the American Chemical Society. 1155 Sixteenth Street N.W., Washington, DC 20036

Single-stage astaxanthin production enhances the non-mevalonate pathway and photosynthetic central metabolism in *Synechococcus* sp. PCC 7002

Tomohisa Hasunuma*[1,2], Ayako Takaki[1], Mami Matsuda[1,2], Yuichi Kato[1,2], Christopher J. Vavricka[2], and Akihiko Kondo[1,2,3]

1. Engineering Biology Research Center, Kobe University, 1-1 Rokkodai, Nada, Kobe 657-8501, Japan

2. Graduate School of Science, Technology and Innovation, Kobe University, 1-1 Rokkodai, Nada, Kobe 657-8501, Japan

3. Biomass Engineering Program, RIKEN, 1-7-22 Suehiro, Tsurumi, Yokohama, Kanagawa 230-0045, Japan

*Correspondence to: Tomohisa Hasunuma (hasunuma@port.kobe-u.ac.jp)

Abstract

The natural pigment astaxanthin is widely used in aquaculture, pharmaceutical, nutraceutical and cosmetic industries due to superior antioxidant properties. The green alga *Haematococcus pluvialis* is currently used for commercial production of astaxanthin pigment. However, slow growing *H. pluvialis* requires a complex two-stage stress-induced process with high light intensity leading to increased contamination risks. In contrast, the fast-growing euryhaline cyanobacterium *Synechococcus* sp. PCC 7002 (*Synechococcus* 7002) is able to reach high density under stress-free phototrophic conditions, and is therefore a promising metabolic engineering platform for astaxanthin production. In the present study, genes encoding β-carotene hydroxylase and β-carotene ketolase, from the marine bacterium *Brevundimonas* sp. SD212, are integrated into the endogenous plasmid of *Synechococcus* 7002, and then expressed to biosynthesize astaxanthin. Although *Synechococcus* 7002 does not inherently produce astaxanthin, the recombinant ZW strain yields 3 mg/g-dry cell weight astaxanthin from CO_2 as the sole carbon source, with significantly higher astaxanthin content than previous cyanobacteria reports. *Synechococcus* 7002 astaxanthin productivity reached 3.35 mg/L/day after just 2 days in a continuous autotrophic process, which is comparable to the best *H. pluvialis* astaxanthin productivities when factoring in growth times. Metabolomics analysis reveals increases in fractions of hexose-, pentose- and triose phosphates along with intermediates involved in the non-mevalonate pathway. Dynamic metabolomics analysis of ^{13}C labeled metabolites clearly indicates flux enhancements in the Calvin cycle and glycolysis resulting from the overexpression

of astaxanthin biosynthetic genes. This study suggests that cyanobacteria may enhance central metabolism as well as the non-mevalonate pathway in an attempt to replenish depleted pigments such as β-carotene and zeaxanthin.

Key words:

Astaxanthin; Carotenoid; Cyanobacteria; Metabolomics; *Synechococcus*

Carotenoids comprise the most diverse type of characterized pigments found in nature. Accordingly, there are widespread applications for carotenoids as food colorants, cosmetics and food additives. Due to high antioxidant activities, carotenoids have become more important for the human health care industry. For instance, carotenoids are reported to protect against premature aging, degenerative diseases and cancers.[1,2]

Among the carotenoids, astaxanthin, a 3,3′-dihydroxylated and 4,4′-diketolated derivative of β-carotene (3,3′-hydroxy-β,β-carotene-4,4′-dione), is one of the most valuable natural products. This pigment has been industrially exploited as a feed dye, particularly as a feed supplement in aquaculture and poultry farming. Astaxanthin is the strongest known antioxidant among carotenoids, due to hydroxy and ketone functional groups at 3,3′- and 4,4′- positions, respectively, with the most positive oxidation potential (relative to the calomel electrode). The diverse biological functions of astaxanthin include involvement in singlet oxygen-quenching, reduction of low-density lipoprotein, anticancer activities, and enhancement of immune responses.[3,4] Thus, the use of astaxanthin in pharmaceutical, nutraceutical and medical applications is expected to dramatically increase.

Currently, the majority of astaxanthin produced for commercial use is chemically synthesized from petrochemical precursors.[5] Chemical synthesis can provide a

steady source of astaxanthin, however there are concerns about the biological functions and safety of synthetic astaxanthin, which is a mixture of (3*S*,3′*R*), (3*R*,3′*R*) and (3*S*,3′*S*) with a proportion ratio of 1:2:1, respectively. The (3*S*,3′*S*) and (3*R*,3′*R*) are most abundant in nature, and these stereoisomers exhibit higher bioactivity than that of synthetic astaxanthin. Additionally, since chemically synthesized astaxanthin might be contaminated with other reaction by-products or intermediates, its use in food additives and pharmaceuticals is not ideal for human consumption. Due to an increase in market demand for natural astaxanthin, systems for biological astaxanthin production have been developed.

The unicellular freshwater green alga *Haematococcus pluvialis* produces the highest reported natural astaxanthin content, and is the primary source for commercial (3*S*,3′*S*) astaxanthin.[6,7] Since *H. pluvialis* biosynthesizes large amounts of astaxanthin under inductive stress conditions such as high light and nitrogen starvation,[8] the alga is cultivated in a two-stage batch process consisting of a growth phase with sufficient nutrient supply and an astaxanthin accumulation phase under stress to induce haematocyst formation. However, slow growth in the first stage and cell deterioration in the second stage increases contamination risks and reduces production periods. In addition, high light irradiation increases production costs. Mixotrophic cultures using acetate supplementation can improve cell growth, but the requirement of additional carbon sources is less sustainable relative to a purely autotrophic system with CO_2 as the sole carbon source. Due to the demand for an economical and environmentally benign production process for

natural astaxanthin, the development of a CO_2 utilizing photoautotrophic systems is ideal.

The euryhaline cyanobacterium *Synechococcus* sp. strain PCC 7002 (hereafter *Synechococcus* 7002) is an attractive chassis for astaxanthin production, as it can achieve high biomass concentrations and unprecedented photoautotrophic biomass productivities (~2.5 h doubling time) compared to the other astaxanthin producers *Synechocystis* sp. PCC 6803 (6.6 h doubling time), *Synechococcus* sp. PCC 7942 (4.9 h doubling time),[9,10,11] and slow growing *H. pluvialis* (6-11 days doubling time).[12] Moreover, *Synechococcus* 7002 is highly resistant to salt and therefore can utilize unprocessed seawater.[9] *Synechococcus* 7002 can naturally synthesize β-carotene and xanthophylls such as zeaxanthin, cryptoxanthin, myxoxanthophyll, echinenone, 3′-hydroxyechinenone and synechoxanthin.[13] Astaxanthin can be biosynthesized from β-carotene via the introduction of ketone and hydroxy groups at the 4,4′ and 3,3′ positions of the β-ionone rings by two enzymes, a β-carotene ketolase and a β-carotene hydroxylase, by way of eight intermediate keto- and/or hydroxy- carotenoids, respectively (Figure 1). Although *Synechococcus* 7002 exhibits both β-carotene hydroxylase and ketolase activities to produce zeaxanthin and 3′-hydroxyechinenone, astaxanthin has never been detected in the wild-type cells. β-carotene ketolases in cyanobacteria were shown to poorly catalyze the conversion of zeaxanthin to astaxanthin via adonixanthin, as it is difficult to accept a 3-hydroxy-β-ionone ring as a substrate.[14,15] Efficient ketolation would be required for the accumulation of astaxanthin in cyanobacteria.

Figure 1 Schematic representation of the designed carotenoid metabolic pathway, resulting from *Brevundimonas crtZ* and *crtW* insertions into the *Synechococcus* 7002 genome. Enzymes are indicated by their gene assignment symbols: CrtR, β-carotene hydroxylase; CrtW, β-carotene ketolase; CrtZ, β-carotene hydroxylase. Abbreviations: DXP, deoxyxylulose 5-phosphate; GAP, glyceladehyde 3-phosphate; MEP, methylerithritol 4-phosphate.

In an *Escherichia coli* complementation study, a *Brevundimonas* sp. SD212 β-carotene ketolase (CrtW) demonstrated efficient introduction of the 4' ketone group of adonixanthin for *in vivo* astaxanthin production.[16] A β-carotene hydroxylase (CrtZ) from the same strain exhibited higher β-carotene conversion efficiency compared to that of CrtZ proteins isolated from other bacteria such as *Pantoea ananatis*, *Paracoccus* spp., *Flavobacterium* sp. and *Thermus thermophilus*.[17] The concurrent expression of *Brevundimonas* sp. SD212 *crtW* and *crtZ*, encoding CrtW and CrtZ, respectively, led to production of more than 5 mg/g astaxanthin in *Nicotiana tabacum* leaves.[18] In the present study, recombinant *Synechococcus* 7002 expressing *crtZ* and *crtW* is developed to increase sustainable astaxanthin production.

Comprehensive metabolomics has identified key metabolites that regulate diverse biological processes.[19,20] By combining temporal metabolomics, *in vivo* metabolite ^{13}C-labeling, and mass distribution analysis, the turnover of intracellular metabolites can be directly and exhaustively observed. We refer to this time-dependent isotope labeling approach as dynamic metabolic profiling or

dynamic metabolomics.[21,22,23] Such profiling enables kinetic visualization of carbon incorporation, partitioning and assimilation in central metabolic pathways such as glycolysis, the pentose phosphate pathway and citric acid cycle.[24,25]

The present study investigates the effects of the *Brevundimonas crtZ* and *crtW* expression on the primary metabolism and astaxanthin production of recombinant *Synechococcus* 7002. Dynamic metabolomics analysis of astaxanthin bioproduction indicates potential bottleneck steps of carotenoid biosynthesis. This enables optimization of astaxanthin production via removal of limiting steps through subsequent metabolic pathway engineering.

Materials and Methods

Strains and culture conditions

The cyanobacterium *Synechococcus* sp. PCC 7002 was grown in medium A2 (4.25 g/L $NaNO_3$, 50 mg/L KH_2PO_4, 18 g/L NaCl, 5 g/L $MgSO_4$ $7H_2O$, 0.37 g/L $CaCl_2$ $2H_2O$, 0.6 g/L KCl, 32 mg/L Na_2EDTA $2H_2O$, 8 mg/L $FeCl_3$ $6H_2O$, 34 mg/L H_3BO_3, 4.3 mg/L $MnCl_2$ $4H_2O$, 0.32 mg/L $ZnCl_2$, 50 µg/L Na_2MoO_4 $2H_2O$, 3.0 µg/L $CuSO_4$ $5H_2O$, 12 µg/ L $CoCl_2$ $6H_2O$, 4.0 µg/L cobalamin, and 8.3 mM tris(hydroxymethyl)aminomethane), slightly modified from medium A.[26] Cyanobacteria were cultured under a fluorescent light source with maximum wavelengths of ~545 nm and ~613 nm. Recombinant cells were pre-cultivated under continuous irradiation with 100 µmol/m^2/s white light photons at 30°C for

2 days. Cells were agitated at 100 rpm in 70 mL of medium A2 containing 100 mg/L kanamycin in closed double-deck flasks with 1% (*v/v*) CO_2, as previously described.[24] The pre-cultured cells were inoculated into fresh medium A2 at an OD_{750} of 0.1 and cultivated for 4 days under 4% (*v/v*) CO_2 and continuous irradiation with 400 μmol/m^2/s white light photons with 100-rpm agitation at 30°C. The cell density in the medium was determined as dry cell weight (DCW) based on the linear correlation between DCW and optical density at 750 nm (OD_{750}) measured with a UV mini spectrophotometer (Shimadzu, Kyoto, Japan).

Construction of recombinant strains

The previously selected homologous recombination site Flank B,[27] was amplified from *Synechococcus* 7002 DNA by PCR using the primers 5'-AAGTGGGGAAACGCGTCTAGACTGTGCCAGATCATA-3'/5'-TGATTACGCCAAGCTT CGAGTAAGCTCGGAATCCCT-3' (restriction enzyme sites are underlined) as a target for homologous recombination. The resulting fragment was integrated into the *Mlu*I and *Hind*III sites of pSKrbcL-slr0168[28] to yield pSKrbcL-FlankB. Another target fragment adjacent to Flank B was designated as Flank 1, and amplified from *Synecococcus* 7002 DNA using the primers, 5'-AGTGAATTCGAGCTCGGTACCATCGCTCTCACCAAAGATTC-3'/5'-CAGCTGGCAATTCCGGCTCGAGGCCTCCTGAATAAATCTATTT-3', followed by integration into the *Kpn*I and *Xho*I sites of pSKrbcL-FlankB to yield pSKrbcL-Flank1-FlankB. A DNA fragment containing *crtZ* and *crtW* genes was amplified from plasmid pLD200-ZW[18] using the primers

5’-GAGGACTGACCTAGCATATGGCTTGGCTTACTTGGATCGC-3’/5’-CCAAAACTGTAACCTGCAGGTCGACTCAAGACTCTCCTCT-3’, and cloned into the *Nde*I and *Sal*I sites of pSKrbcL-Flank1-FlankB to yield pSKrbcL-Flank1-FlankB/crtZW. The *psbA2* promoter was amplified from *Synechocystis* 6803 DNA using the primers 5’-TTCTTCTGAGCGGCCGCTCATTATTTCATCTCCATTGTCC-3’/5’-TCGACTCTAGACATATGGGTTATAATTCCTTATGTATTTGTC-3’, followed by ligation into the *Not*I and *Nde*I sites of pSKrbcL-Flank1-FlankB and pSKrbcL-Flank1-FlankB/crtZW to yield pSKrbcL-Flank1-FlankB and pSKpsbA2-Flank1-FlankB/crtZW, respectively.

Wild-type *Synechococcus* 7002 was transformed with pSKpsbA2-Flank1-FlankB/crtZW and pSKrbcL-Flank1-FlankB to yield strain ZW and the control strain CT, respectively. Cells of mid-exponential phase cultures (OD_{750} of approximately 1.0) were suspended in 100 µL of medium A2, and mixed with less than 10 µL of plasmid solution containing 3,000-6,000 ng plasmid in a test tube. 10-20 µL of the mixture was then spread onto 0.45-µm pore size nitrocellulose membrane filter (Millipore, Billerica, MA) placed on a medium A2 plate. After cultivation at 30 °C under continuous white light for 2 days, the membrane filter was transferred onto a medium A2 plate containing 50 mg/L kanamycin. Single colony isolation was repeated to achieve complete segregation of *Synechococcus* 7002 with integration of *crtZ* and *crtW* genes, and the plasmid-derived sequence into the most abundant endogenous plasmid pAQ-1 with a copy number of ~50. Correct integration into pAQ-1 was confirmed by PCR

using the specific primer set 5'-GGCTTTGTATTTAAGCCGGATATCAACAGGCG-3'/5'-CCTCCTAGGGGCGCTCAAAG GTGATAATTAT-3'.

Metabolome analysis

Samples for metabolome analysis were prepared according to a previous method[24] with modifications. Culture medium containing 5 mg DCW of cells were mixed with pre-cooled (30°C) 32.5% (*v*/*v*) methanol, with a culture medium to methanol solution ratio of 1:4. After centrifugation at 8,000 *g* for 3 min with a temperature setting of -4°C, unfrozen methanolic supernatant was removed. After washing cells with 20 mM ammonium bicarbonate (pH 8.7), cells were immediately suspended in 1 mL of pre-cooled methanol containing 37.38 μM methionine sulfone and 37.38 μM piperazine-1,4-bis(2-ethanesulfonic acid) as internal standards for mass analysis. 0.5 mL of cell suspension was mixed with 0.2 mL of water pre-cooled at 4°C and 0.5 mL of chloroform on ice. After mixing for 30 s, layer separation was performed by centrifugation at 14,000 *g* for 5 min at 4°C. 500 μL of aqueous layer was filtered through a 3 kDa cut-off membrane (Millipore), and then evaporated under vacuum. The dried extract of metabolites was dissolved in Milli-Q water. Metabolite analysis was performed with a capillary electrophoresis-mass spectrometry (CE-MS) system (Agilent Technologies, Palo Alto, CA) as described previously.[24]

Pigment analysis

Cell sampling was performed according to a previously reported method[22] with minor modifications. Cyanobacterial cells equivalent to 5 mg DCW were collected by centrifugation at 8,000 *g* for 3 min at 4°C. After washing with 20 mM ammonium bicarbonate (pH 8.7), collected cells were suspended in 1 mL of pre-cooled (-30°C) methanol, and then 300 µL of pre-cooled (-30°C) chloroform and 100 µL of pre-cooled (4°C) water was added into the cell suspension. After voltexing for 1 min and sonication for 5 min, the cell suspension was shaken at 1200 rpm (MBR-022UP; TAITEC, Saitama, Japan) for 30 min at 4°C in the dark before centrifugation at 14,000 *g* for 5 min at 4°C. 980 µL of cell extract obtained as the supernatant was transferred to a clean tube. After adding 440 µL of water, phase separation of aqueous and organic layers was performed by centrifugation at 14,000 *g* for 5 min at 4°C. A 50 µL aliquot of the organic layer obtained as a pigment extract was diluted to a final volume of 500 µL with a solution of 8:2 (*v*/*v*) acetonitrile:chloroform containing 0.75 µM trans-β-apo-8'-carotenal as an internal standard for the quantification analysis. Carotenoids and chlorophyll *a* were quantified with an Acquity ultra performance liquid chromatography (UPLC) system (Waters Corporation, Milford, MA) equipped with a photodiode array (PDA) detector as described previously.[18]

Dynamic ^{13}C-labeling metabolomics

In-vivo ^{13}C-labeling metabolomics was performed to analyze the turnover of intracellular metabolites. *Synechococcus* cells were cultivated for 72 h in medium

A2 under 400 μmol photons/m^2/s light intensity and 4% (v/v) CO_2 conditions at 30°C. 15 mL of cell suspension was centrifuged at 10,000 *g* for 5 min at 30°C. After the removal of supernatant, cells were re-suspended in medium A2 containing 25 mM ^{13}C-sodium bicarbonate. After labeling for 0-30 min under the same light intensity of 400 μmol photons/m^2/s at 30°C, cells were collected by centrifugation, metabolites were extracted, and then extracts were applied to CE-MS metabolome analysis as described above. Mass shifts from ^{12}C to ^{13}C by ^{13}C-incorporation into metabolites were observed in the mass spectra. ^{13}C fractions, defined as the ratios of ^{13}C to total carbon, were calculated by relative isotopomer abundance ratios (m_i) of metabolites incorporating i^{13}C atoms as follows:

$$m_i(\%) = \frac{M_i}{\sum_{j=0}^{n} M_j} \times 100$$

$$^{13}\text{C fraction}\,(\%) = \sum_{i=1}^{n} \frac{i \times m_i}{n}$$

where M_i represents the isotopomer abundance of metabolite incorporating i^{13}C atoms, and *n* is the number carbon atoms in the metabolite.

Photosynthesis analysis

Synechococcus cells were cultivated in medium A2 under 400 μmol photons/m^2/s light intensity and 4% (v/v) CO_2 conditions at 30°C. After 48 h cultivation, photosynthesis analysis was carried out. Oxygen evolution was measured with an oxygen electrode (Hansatech, King's Lynn, UK). For the measurement, a reaction mixture (2 mL) containing 10 mM $NaHCO_3$ and cells (10 μg chlorophyll/mL) was

first incubated in the dark for 10 min under air-equilibrated conditions, followed by illumination with halogen light at 400 μmol photons/m^2/s at 30°C. During the measurements, the reaction was mixed with a magnetically controlled micro-stirrer.

Electron microscopy

Ultrastructures of *Synechococcus* cells cultivated for 72 h under 400 μmol photons/m^2/s light intensity and 4% (*v/v*) CO_2 conditions at 30°C were observed using transmission electron microscopy (TEM) by Tokai Electron Microscope, Inc. Briefly, cell samples were fixed, dehydrated with ethanol, infiltrated with propylene oxide and polymerized in resin. Ultra-thin sections were cut, stained and then observed with a JEM-1400Plus.

Results

Construction of recombinant *Synechococcus* 7002 cells

The genes *crtZ* and *crtW* from *Brevundimonas* sp. are arranged as an operon under the control of a *psbA2* promoter between Flank 1 and Flank B, which function as anchoring regions for site-specific integration into the *Synechococcus* 7002 plasmid pAQ1[27] through homologous recombination (Figure 2a). Transformation of wild-type *Synechococcus* 7002 with expression vector pSKpsbA2-Flank1-FlankB/crtZW resulted in strain ZW. Transformation of *Synechococcus* 7002 with the empty vector pSKpsbA2-Flank1-FlankB resulted in

insertion of the kanamycin resistance cassette into pAQ1 of the marker control strain (CT). Heterologous genes are correctly integrated and segregated as verified by PCR (Figure 2b).

Figure 2 Molecular characterization of the parental (WT), *crtZ*/*crtW*-overexpressing (ZW), and marker control (CT) strains. (a) Genome structure around homologous recombination sites in WT, ZW and CT strains. Km^r, kanamycin resistance cassette; P_{psbA2}, *psbA2* promoter; T_{rbcL}, *rbcL* promoter. (b) Genomic PCR analysis of WT, ZW and CT strains using Pr1 and Pr2.

Pigment production in recombinant *Synechococcus* 7002 cells

Figure 3a shows phototrophic growth of strain CT and ZW cells, using continuous irradiation with 400 μmol photons/m^2/s light intensity and 4% (v/v) CO_2 at 30°C. There is no significant difference between CT and ZW cells. After 96-h cultivation, cell concentration of ZW is 4.49 g-DCW/L, while that of CT is 4.60 g-DCW/L.

Figure 3 Effect of *crtZ*/*crtW* expression on cell growth and pigment production of *Synechococcus* 7002. (a) Time course of cellular biomass. (b) Plot of OD_{750} vs. cellular biomass. Values in panels a and b represent the average (± SD) of three independent experiments. (c) Difference in color between ZW and CT. (d) Absorption spectra of ZW (red) and CT (black) cultivated for 96 h under 400 μmol photons/m^2/s light intensity and 4% CO_2 conditions.

ZW cells exhibit a darker green color compared to CT cells (Figure 3b). Figure 3c shows absorption spectra for the recombinant strains cultivated for 96 h. Four peaks are assigned to the chlorophyll Soret (~435 nm), carotenoid (~500 nm), phycobilisome (~620 nm), and chlorophyll Qy(0,0) (~676 nm) bands.[29] The expression of *crtZ* and *crtW* results in a decrease in absorbance at 435 nm and 676 nm, indicating a decrease in chlorophyll *a*. On the other hand, the increase in the absorbance at 500 nm and 620 nm is observed which indicates an increase in total carotenoid and phycobilisome, respectively.

Each pigment compound is quantified by UPLC-PDA. CT accumulates zeaxanthin, chlorophyll *a* and β-carotene as major pigments, while ZW cells are found to accumulate astaxanthin, adonixanthin, adonirubin and hydroxylechinenone, which are all not detected in CT cells (Figure 4a). In the chromatogram, several peaks are observed only in ZW at 3.81, 4.05, 6.06 and 6.15 min. According to their ultraviolet-visible absorption spectra (Supplementary Figure 1), these peaks correspond to carotenoids. Chlorophyll *a* content of ZW is lower than that of CT. Zeaxanthin and β-carotene levels are drastically reduced by the expression of *crtZ* and *crtW* (Figure 4b). Instead, ZW produces approximately 3 mg/g-DCW astaxanthin. Adonixanthin, adonirubin, hydroxyechinenone and echinenone are produced as minor pigments in ZW. Productivity of astaxanthin converted from CO_2 is 3.35 mg/L/day from 48 h to 96 h.

Figure 4 Effect of *crtZ*/*crtW* expression on pigment production of *Synechococcus* 7002. (a) A_{450} chromatograph obtained with UPLC-PDA. Pigments are extracted from cells cultivated for 96 h under 400 μmol photons/m^2/s light intensity and 4% CO_2 conditions. Abbreviations: Ast, astaxanthin; Adx, adonixanthin; Adr, adonirubin; Z, zeaxanthin; IS, internal standard; HE, hydroxyechinenone; E, echinenone; Chl *a*, chlorophyll *a*; β-Car, β-carotene; UI, unidentified compound. (b) Time course of pigment level in ZW and CT cultivated under 400 μmol photons/m^2/s light intensity and 4% CO_2 conditions. Values represent the average (± SD) of three independent experiments.

Photosynthesis and morphology of astaxanthin-producing cells

β-carotene and zeaxanthin participate in light harvesting and energy transfer to chlorophyll and photoprotection, and are thought to be essential components of the photosynthesis apparatus of cyanobacteria. Therefore, alteration of the carotenoid composition might affect photosynthetic activity of recombinant cells. Although expression of *crtZ* and *crtW* drastically decrease β-carotene and zeaxanthin, there is no significant difference in the oxygen evolution rate between ZW and CT strains (p-values over 0.17) (Figure 5). According to TEM analysis, ZW cells are longer than wild-type cells (Supplementary Figure 2). In ZW cells, granules visible between thylakoid membrane of wild-type cells disappear.

Figure 5 Light response for O_2 evolution rate in ZW and CT cultivated for 28 and 48 h under 400 μmol photons/m^2/s light intensity and 4% CO_2 conditions. Values represent the average (± SD) of three independent experiments.

Time-course metabolome in *crtZ*/*crtW*-expressing cells

Increases in astaxanthin, echinenone, hydroxyechinenone, adonirubin, and adonixanthin (Figure 4) raises the possibility that the carotenoid precursor supply is enhanced by the expression of *crtZ* and *crtW*. Thus, time-course alteration in the pool size of hydrophilic metabolites involved in central metabolism including the Calvin cycle and glycolysis as well as the 2-*C*-methyl-D-erithritol 4-phosphate (MEP) pathway are measured with CE coupled to MS for the efficient determination of highly polar molecules (Figure 6).

Figure 6 Time course of intracellular metabolite pool size in ZW and CT. Values represent the average (± SD) of three independent experiments. Abbreviations: CDP-ME, 4-diphosphocytidyl-2-*C*-methylerythritol; DXP, 1-deoxy-D-xylulose 5-phosphate; MEcPP, 2-C-methylerythritol 2,4-cyclodiphosphate; MEP, 2-*C*-methylerythritol 4-phosphate; FBP, fructose 1,6-bisphosphate; F6P, fructose 6-phosphate; PEP, phosphoenolpyruvate; HMBPP, (*E*)-4-hydroxy-3-mehyl-but-2-enyl pyrophosphate; 2PGA, 2-phosphoglycerate; 3PGA, 3-phosphoglycerate; R5P, ribulose 5-phosphate; RuBP, ribulose 1,5-bisphosphate; Ru5P, ribulose 5-phosphate; S7P, sedoheptulose 7-phosphate.

In the MEP pathway, although 1-deoxy-D-xylulose 5-phosphate (DXP) is below the detection limit in the CT strain, the ZW strain accumulates more than 10 nmol/g-DCW of DXP. Pool size of 2-*C*-methyl-D-erythritol 2,4-cyclodiphosphate

(MEcPP) and (*E*)-4-hydroxy-3-methyl-but-2-enyl pyrophosphate (HMBPP) are higher in ZW than in CT. Regarding metabolites involved in the Calvin cycle and glycolysis, ZW shows higher accumulation of ribose 5-phosphate (R5P), ribulose 5-phosphate (Ru5P), ribulose 1,5-bisphosphate (RuBP), fructose 1,6-bisphosphate (FBP), 3-phosphoglycerate (3PGA), and 2-phosphoglycerate (2PGA), phosphoenolpyruvate (PEP), after 48 h cultivation relative to that of CT. After 96 h, Ru5P, RuBP, FBP and 3PGA levels are still higher in ZW than in CT. These pool size data indicate alterations in the metabolism of carotenoid precursors result from the expression of *crtZ* and *crtW* genes.

Dynamic metabolism determined by ^{13}C-labeling metabolomics

Pool size analysis of intermediate metabolite is insufficient to account for carbon flow and distribution, because metabolite amount depends on the rate of synthesis and decomposition of the metabolite. Even if a particular reaction is activated in metabolism, the amount of metabolite could remain unchanged under steady state conditions. Thus, in order to elucidate the effects of *crtZ*/*crtW* expression on the carbon flux of central metabolism, kinetics of carbon assimilation is determined by an *in vivo* ^{13}C-labeling assay with $NaH^{13}CO_3$.

The dynamic metabolic profiling, shown in Figure 7, reveals that the turnover of central metabolites F6P, 3PGA, PEP and S7P is higher in ZW than in CT. Turnover of G6P and FBP is also observed to be higher in ZW (Table 1). The ^{13}C fraction is defined as the ratio of ^{13}C to total carbon in metabolites, which is estimated from

the distribution of mass isotopomers detected by mass spectrometry. The initial slope of the ^{13}C-fraction *versus* time curve reflects the turnover rate of metabolites (Table 1). This data shows that the carbon flow of central metabolism is enhanced by the *crtZ*/*crtW* expression. Note that the ^{13}C fraction of pyruvate and MEP pathway intermediates cannot be evaluated because of their low abundance in cells.

Figure 7 Time-course changes in ^{13}C fractions of various metabolites in ZW and CT. Values represent the average (± SD) of three independent experiments.

Table 1 ^{13}C fraction initial slopes and pool sizes (μmol/g-DCW) for central metabolites.

	ZW Slope	CT Slope	ZW Pool size	CT Pool size
F6P	8.22 (0.838)	4.36 (1.55)	0.038 (0.009)	0.035 (0.004)
FBP	7.78 (0.729)	5.63 (1.58)	0.037 (0.006)	0.006 (0.001)
G6P	8.11 (0.916)	4.21 (1.51)	0.078 (0.01)	0.061 (0.006)
PEP	9.16 (0.424)	6.66 (0.952)	0.183 (0.009)	0.044 (0.006)
3PGA	8.54 (0.512)	6.48 (0.903)	4.33 (0.565)	0.655 (0.093)
S7P	9.28 (0.854)	6.287 (1.35)	0.325 (0.059)	0.276 (0.013)

Slopes were calculated from 0 - 5 min. Standard deviations are given in parenthesis with all values based on three independent measurements (n = 3).

Discussion

Recombinant cyanobacteria were first reported to produce astaxanthin and other ketocarotenoids via addition of an algal P-C-4-oxygenase to *Synechococcus* PCC 7942, and later *Synechococcus* PCC 6803.[30,31]

In the current study, the faster growth rate of *Synechococcus* PCC 7002 led to improved cyanobacteria astaxanthin titers of 3 mg/g-dry cell weight from CO_2, with a productivity of 3.35 mg/L/day. Higher *H. pluvialis* astaxanthin productivity has been reported at 17 mg/L/day, but this requires a slow two-step process with a green phase of 10-11 days followed by an 11-12 day red phase.[32,33,34] In contrast, the maximum *Synechococcus* 7002 productivity is reached after just 2 days in a continuous photoautotrophic process. *H. pluvialis* astaxanthin productivity could be scaled up from 2.5 mg/L/day to 10.5 mg/L/day by changing from Erlenmeyer flasks to a bubbling column photobioreactor.[34] This encourages the improvement of *Synechococcus* 7002 titers by changing to bubbling bioreactors.

H. pluvialis carotenoid production under stress conditions can stimulate central metabolism,[35] but this may also slow down cell division and photosynthesis.[36] Although the regulation of cyanobacteria carotenoid related pathways have been investigated using a variety of genetic approaches,[37,38,39,40,41] the metabolic bottlenecks have remained unclear. By including dynamic metabolomic profiling in the current study, increases in flux through central metabolism could be observed to accompany astaxanthin production in *Synechococcus* PCC 7002. However, total carotenoid and chlorophyl content remained approximately two-fold lower relative to the control strain. The increase in central metabolism flux balanced with decreases in flux to pigments (Figure 4) is consistent with the similar rates of oxygen evolution in the ZW and CT strains, and supports a hypothesis that increased central metabolism is needed to compensate for the lack of light

harvesting pigments. Furthermore, the ultraviolet-visible absorbance spectrum (Figure 3d) of the ZW strain shows a relative increase around ~620 nm, which might indicate that expression of phycocyanin antenna protein production is upregulated to help compensate for the loss of other light harvesting pigments. Although growth rates were not affected during recombinant astaxanthin production, the increased cell length could be related to the enhanced central metabolism or possibly changes in the circadian cycle due to altered pigment composition.[42]

Cyanobacteria terpenoids, which include carotenoids, sterols, ubiquinones, sesquiterpenes and many others, are all produced via the MEP pathway.[43] The time course metabolomics analyses show increases in flux from central metabolism through the MEP pathway during astaxanthin production in *Synechococcus* PCC 7002. The pool sizes of non-mevalonate pathway intermediates DXP, CDP-ME, MEcPP and HMBPP were higher in the ZW strain as shown in Figure 6. The observed increases in the pool sizes of DXP indicate that there is enhanced metabolic flux from pyruvate to DXP, together with a remaining astaxanthin bottleneck from DXP to MEP. Therefore, overexpression of DXP reductoisomerase to increase turnover of DXP to MEP is a good option to increase production of astaxanthin and other terpenoids.

Carotenoid composition can have diverse effects on various host strains.[8,44] In microalgae, astaxanthin can protect against multiple stresses, including

photooxidative damage, and further participate in light harvesting complexes.[36] In cyanobacteria, including *Synechococcus* 7002, the 3′-hydroxyechinenone binding orange carotenoid protein may protect against the photodamage of phycobilisomes.[45,46] Therefore, the observed increase of 3′-hydroxyechinenone in the ZW strain suggests that phycobilisome interactions might be related to enhancement of photosynthetic central metabolism. In conclusion, this work establishes the green cyanobacteria *Synechococcus* 7002 as a fast growing photoautotrophic carotenoid production chassis, and provides a framework for future improvement of carotenoid synthetic bioproduction studies.

Supporting Information

Supporting Information is included as a separate PDF document. Ultraviolet-visible absorption spectra of UPLC-PDF peaks and TEM micrographs are included as additional figures.

Author Contributions

TH designed the experiments. AT and MM performed the experiments. TH, AT, MM, YK and CJV analyzed the data. TH and CJV wrote the manuscript.

Acknowledgements

The authors thank Ms. Ryoko Yamazaki for technical assistance.

Funding Sources

This work was supported by JSPS KAKENHI Grant Number JP15H05557 to TH. TH is also supported by the Advanced Low Carbon Technology Research and Development Program (ALCA, JPMJAL1306) from the Japan Science and Technology Agency (JST), the Ministry of Education, Culture, Sports, Science, and Technology (MEXT), Japan. CJV is additionally supported by JSPS KAKENHI (V18K065770) and Kato Memorial Bioscience Foundation (2017M-014).

References

(1) Fiedor, J., Burda, K. (2014) Potential role of carotenoids as antioxidants in human health and disease. *Nutrients 6*, 466-488.

(2) Krinsky, N. I., Johnson, E. J. (2005) Carotenoid actions and their relation to health and disease. *Mol. Asp. Med. 26*, 459–516.

(3) Hussein, G., Sankawa, U., Goto, H., Matsumoto, K., Watanabe, H. (2006) Astaxanthin, a carotenoid with potential in human health and nutrition. *J. Nat. Prod. 69*, 443-449.

(4) Ohgami, K., Shiratori, K., Kotake, S., Nishida, T., Mizuki, N., Yazawa, K., Ohno, S. (2003) Effects of astaxanthin on lipopolysaccharide-induced inflammation in vitro and in vivo. *Investig. Ophthalmol. Vis. Sci. 44*, 2694–2701.

(5) Li, J., Zhu, D., Niu, J., Shen, S., Wang, G. (2011) An economic assessment of astaxanthin production by large scale cultivation of *Haematococcus pluvialis*. *Biotechnol. Adv. 29*, 568–574.

(6) Lorenz, R. T., Cysewski, G. R. (2000) Commercial potential for *Haematococcus* microalgae as a natural source of astaxanthin. *Trends. Biotechnol. 18*, 160-167.

(7) Shah, M. M. R., Liang Y., Cheng, J. J., Daroch, M. (2016) Astaxanthin-producing green microalga *Haematococcus pluvialis*: from single cell to high value commercial products. *Front. Plant Sci. 7*, 531.

(8) Mulders, K. J. M. (2014) Phototrophic pigment production with microalgae: biological constraints and opportunities. *J. Phycol. 50*, 229-242.

(9) Aikawa, S., Nishida, A., Ho, S.-H., Chang, J.S., Hasunuma, T., Kondo, A. (2014) Glycogen production for biofuels by the euryhaline cyanobacteria *Synechococcus* sp strain PCC 7002 from an oceanic environment. *Biotechnol. Biofuels 7*, 88.

(10) Yu, J., Liberton, M., Cliften, P. F., Head, R. D., Jacobs, J. M., Smith, R. D., Koppenaal, D. W, Brand, J. L., Pakrasi, H. B. (2015) *Synechococcus elongatus* UTEX 2973, a fast growing cyanobacterial chassis for biosynthesis using light and CO_2. *Sci. Rep. 5*, 8132.

(11) Bernstein, H. C., McClure, R. S., Hill, E. A., Markillie, L. M., Chrisler, W. B., Romine, M. F., McDermott, J. E., Posewitz, M. C., Bryant, D. A., Konopka, A. E., Fredrickson, J. K., Beliaev, A. S. (2016) Unlocking the constraints of cyanobacterial productivity: acclimations enabling ultrafast growth. *mBio 2*, e00181-16.

(12) Sipauba-Tavares, L. H., Berchielli-Morais, F. A., Scardoeli-Truzzi, B. (2015) Growth of *Haematococcus pluvialis* Flotow in alternative media. *Braz. J. Biol. 75*, 796-803.

(13) Zhu, Y., Graham, J. E., Ludwig, M., Xiong, W., Alvey, R. M., Shen, G., Bryant, D. A. (2010) Roles of xanthophyll carotenoids in protection against photoinhibition and oxidative stress in the cyanobacterium *Synechococcus* sp. strain PCC 7002. *Arch. Biochem. Biophys. 504*, 86-99.

(14) Choi, S.-K., Harada, H., Matsuda, S., Misawa, N. (2007) Characterization of two β-carotene ketolases, CrtO and CrtW, by complementation analysis in *Escherichia coli*. *Appl. Microbiol. Biotechnol. 75*, 1335–1341.

(15) Tsuchiya, T., Takaichi, S., Misawa, N., Maoka, T., Miyashita, H., Mimuro, M. (2005) The cyanobacterium *Gloeobacter violaceus* PCC 7421 uses bacterial-type phytoene desaturase in carotenoid biosynthesis. *FEBS Lett. 579*, 2125–2129.

(16) Choi, S.-K., Nishida, Y., Matsuda, S., Adachi, K., Kasai, H., Peng, X., Komemushi, S., Miki, W., Misawa, N. (2005) Characterization of β-carotene ketolases, CrtW, from marine bacteria by complementation analysis in *Eschericia coli*. *Mar. Biotechnol. 7*, 515–522.

(17) Choi, S.-K., Matsuda, S., Hoshino, T., Peng, X., Misawa, N. (2006) Characterization of β-carotene 3,3′-hydroxylases, CrtZ, and P450 in astaxanthin biosynthetic pathway and adonirubin production by gene combination in *Eschericia coli*. *Appl. Microbiol. Biotechnol. 72*, 1238–1246.

(18) Hasunuma, T., Miyazawa, S.-I., Yoshimura, S., Shinzaki, Y., Tomizawa, K.-I., Shindo, K., Choi, S.-K., Misawa, N., Miyake, C. (2008) Biosynthesis of astaxanthin in tobacco leaves by transplastomic engineering. *Plant J. 55*, 857-868.

(19) Diamond, S., Jun, D., Rubin, B. E., Golden, S. S. (2015) The circadian oscillator in *Synechococcus elongatus* controls metabolite partitioning during diurnal growth. *Proc. Natl. Acad. Sci. U S A 112*, E1916-1925.

(20) Link, H., Kochanowski, K., Sauer, U. (2013) Systematic identification of allosteric protein-metabolite interactions that control enzyme activity *in vivo*. *Nat. Biotechnol. 31*, 357-361.

(21) Hasunuma, T., Harada, K., Miyazawa, S., Kondo, A., Fukusaki, E., Miyake, C. (2010) Metabolic turnover analysis by a combination of *in vivo* ^{13}C-labeling from ^{13}CO2 and metabolic profiling with CE-MS/MS reveals rate-limiting steps of the C_3 photosynthetic pathway in *Nicotiana tabacum* leaves. *J. Exp. Bot. 61*, 1041-1051.

(22) Hasunuma, T., Kikuyama, F., Matsuda, M., Aikawa, S., Izumi, Y., Kondo, A. (2013) Dynamic metabolic profiling of cyanobacterial glycogen biosynthesis under conditions of nitrate depletion. *J. Exp. Bot. 64*, 2943-2954.

(23) Vavricka, C. J., Hasunuma, T., Kondo, A. (2019) Dynamic metabolomics for engineering biology: accelerating learning cycles for bioproduction. *Trends Biotechnol. In Press*.

(24) Hasunuma, T., Matsuda, M., Senga, Y., Aikawa, S., Toyoshima, M., Shimakawa, G., Miyake, C., Kondo, A. (2014) Overexpression of flv3 improves photosynthesis in the cyanobacterium *Synechocystis* sp. PCC 6803 by enhancement of alternative electron flow. *Biotechnol. Biofuels 7*, 493.

(25) Hasunuma, T., Matsuda, M., Kato, Y., Vavricka, C. J., Kondo. A. (2018) Temperature enhanced succinate production concurrent with increased central metabolism turnover in the cyanobacterium *Synechocystis* sp. PCC 6803. *Metab. Eng. 48*, 109-120.

(26) Ludwig, M., Bryant, D. A. (2011) Transcription profiling of the model cyanobacterium *Synechococcus* sp. PCC 7002 by Next-Gen (SOLiDTM) sequencing of cDNA. *Front. Microbiol. 2*, 41.

(27) Xu, Y., Alvey, R. M., Byrne, P. O., Graham, J. E., Shen, G., Bryant, D. A. (2011) Expression of genes in cyanobacteria: adaptation of endogenous plasmids as platforms for high-level gene expression in *Synechococcus* sp. PCC 7002. *Methods Mol. Biol. 684*, 273-293.

(28) Hasunuma, T., Matsuda, M., Kondo. A. (2016) Improved sugar-free succinate production by *Synechocystis* sp. PCC 6803 following identification of the limiting steps in glycogen catabolism. *Metab. Eng. Commun. 3*, 130-141.

(29) Akimoto, S., Yokono, M., Hamada, F., Teshigahara, A., Aikawa, S., Kondo, A. (2012) Adaptation of light-harvesting systems of *Arthrospira platensis* to light conditions, probed by time-resolved fluorescence spectroscopy. *Biochim. Biophys. Acta 1817*, 1483–1489.

(30) Harker M., Hirschberg, J. (1997) Biosynthesis of ketocarotenoids in transgenic cyanobacteria expressing the algal gene for β-C-4-oxygenase, *crtO*. *FEBS Lett. 404*, 129-134.

(31) Menin, B., Santabarbara, S., Lami, A., Musazzi, S., Monteleone, F. V., Casazza, A. P (2019) Non-endogenous ketocarotenoid accumulation in engineered *Synechocystis* sp. PCC 6803. *Physiol. Plant. 166*, 403-412.

(32) Wang, J., Han, D., Sommerfeld, M. R., Lu, C., Hu, Q. (2013) Effect of initial biomass density on growth and astaxanthin production of *Haematococcus pluvialis* in an outdoor photobioreactor. *J. Appl. Phycol. 25*, 253-260.

(33) Wang, J., Sommerfeld, M. R., Lu, C., Hu, Q. (2013) Combined effect of initial biomass density and nitrogen concentration on growth and astaxanthin production of *Haematococcus pluvialis* (Chlorophyta) in outdoor cultivation. *Algae 28*, 193-202.

(34) Zhang Z., Wang, B., Hu, Q., Sommerfeld, M., Li, Y., Han, D. (2016) A new paradigm for producing astaxanthin From the unicellular green alga *Haematococcus pluvialis*. *Biotechnol. Bioeng. 113*, 2088-2099.

(35) Recht, L., Töpfer, N., Batushansky, A., Sikron, N., Gibon, Y., Fait, A., Nikoloski, Z., Boussiba, S., Zarka, A. (2014) Metabolite profiling and integrative modeling reveal metabolic constraints for carbon partitioning under nitrogen starvation in the green algae *Haematococcus pluvialis. J Biol. Chem. 289*, 30387-30403.

(36) Solovchenko, A. E. (2015) Recent breakthroughs in the biology of astaxanthin accumulation by microalgal cell. *Photosynth. Res. 125*, 437-449.

(37) Cazzonelli, C. I., Pogson, B. J. (2010) Source to sink: regulation of carotenoid biosynthesis in plants. *Trends Plant Sci. 15*, 266-74.

(38) Englund, E., Andersen-Ranberg, J., Miao, R., Hamberger, B., Lindberg, P. (2015) Metabolic engineering of *Synechocystis* sp. PCC 6803 for production of the plant diterpenoid manoyl oxide. *ACS Synth Biol. 4*, 1270-8.

(39) Choi, S. Y., Lee, H. J., Choi, J., Kim, J., Sim, S. J., Um, Y., Kim, Y., Lee, T. S., Keasling, J. D., Woo, H. M., (2016) Photosynthetic conversion of CO_2 to farnesyl diphosphate-derived phytochemicals (amorpha-4,11-diene and squalene) by engineered cyanobacteria. *Biotechnol Biofuels. 9*, 202.

(40) Kudoh, K., Hotta, S., Sekine, M., Fujii, R., Uchida, A., Kubota, G., Kawano, Y., Ihara, M. (2017) Overexpression of endogenous 1-deoxy-d-xylulose 5-phosphate synthase (DXS) in cyanobacterium *Synechocystis* sp. PCC 6803 accelerates protein aggregation. *J. Biosci. Bioeng. 123*, 590-596.

(41) Zhai, S., Xia, X., He, Z. (2016) Carotenoids in staple cereals: metabolism, regulation, and genetic manipulation. *Front. Plant Sci. 10*, 1197.

(42) Martins B., M., C., Tooke, A., K., Thomas, P., Locke, J. C. W. (2018) Cell size control driven by the circadian clock and environment in cyanobacteria. *Proc. Natl. Acad. Sci. U S A 115*, E11415-E11424.

(43) Pattanaik, B., Lindberg, P. (2015) Terpenoids and their biosynthesis in cyanobacteria. *Life 5*, 269-293.

(44) Erickson, E., Wakao, S., Niyogi, K. K. (2015) Light stress and photoprotection in *Chlamydomonas reinhardtii*. *Plant J. 82*, 449-65.

(45) Bryant, D. A., de Lorimier, R., Guglielmi, G., Stevens Jr., S. E. (1990) Structural and compositional analyses of the phycobilisomes of *Synechococcus* sp. PCC 7002. Analyses of the wild-type strain and a phycocyanin-less mutant constructed by interposon mutagenesis. *Arch. Microbiol.153*, 550-60.

(46) Harris, D., Tal, O., Jallet, D., Wilson, A., Kirilovsky, D., Adir, N. (2016) Orange carotenoid protein burrows into the phycobilisome to provide photoprotection. *Proc. Natl. Acad. Sci. U. S. A. 113*, E1655-E1662.

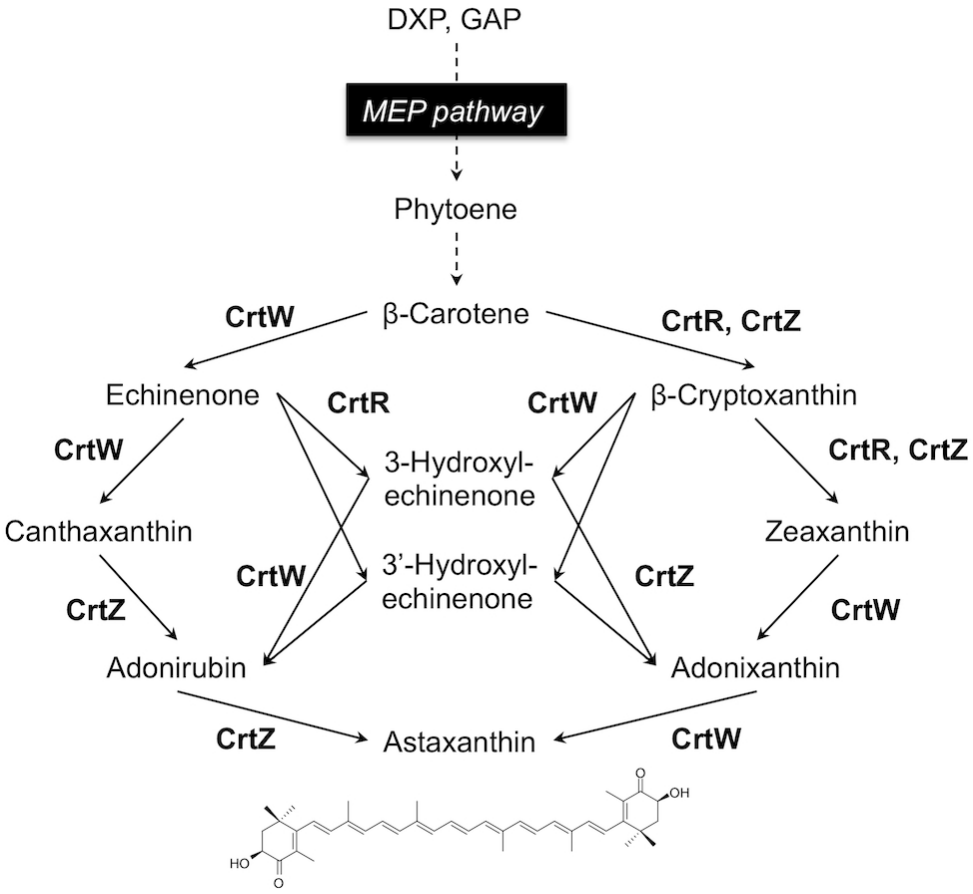

Figure 1

84x75mm (300 x 300 DPI)

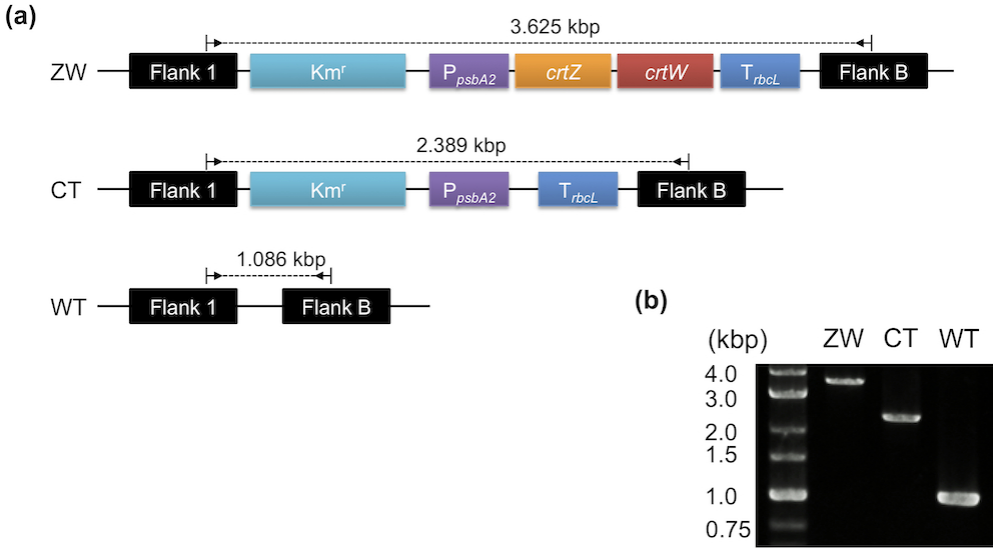

Figure 2

84x47mm (300 x 300 DPI)

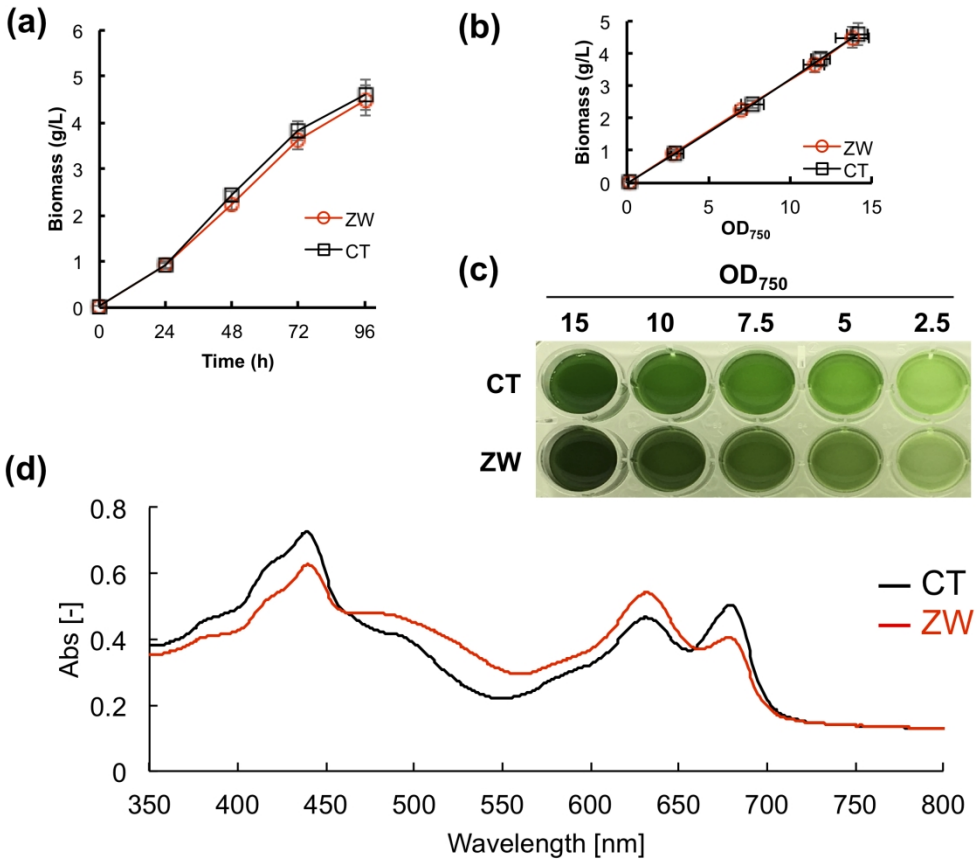

Figure 3

186x166mm (300 x 300 DPI)

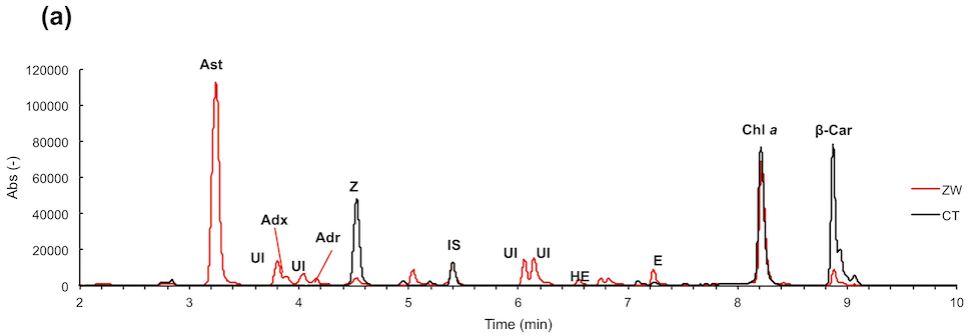

Figure 4a

84x30mm (300 x 300 DPI)

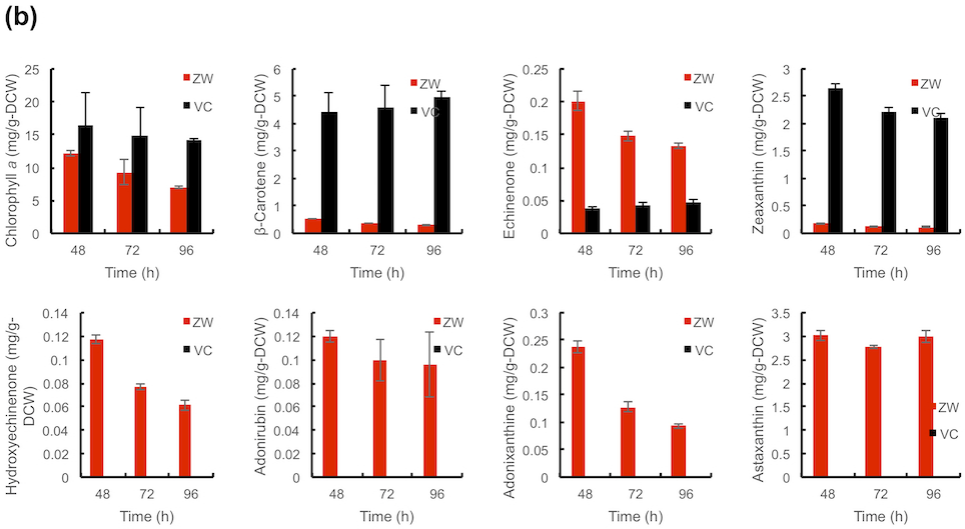

Figure 4b

84x46mm (300 x 300 DPI)

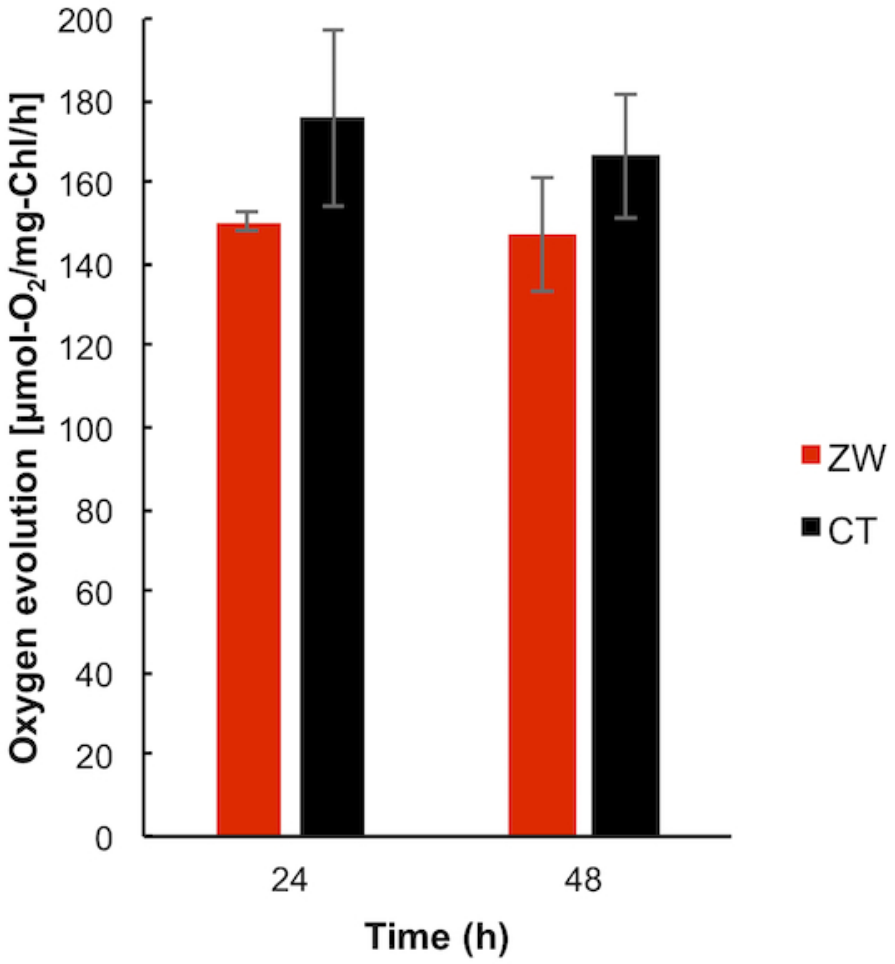

Figure 5

50x53mm (300 x 300 DPI)

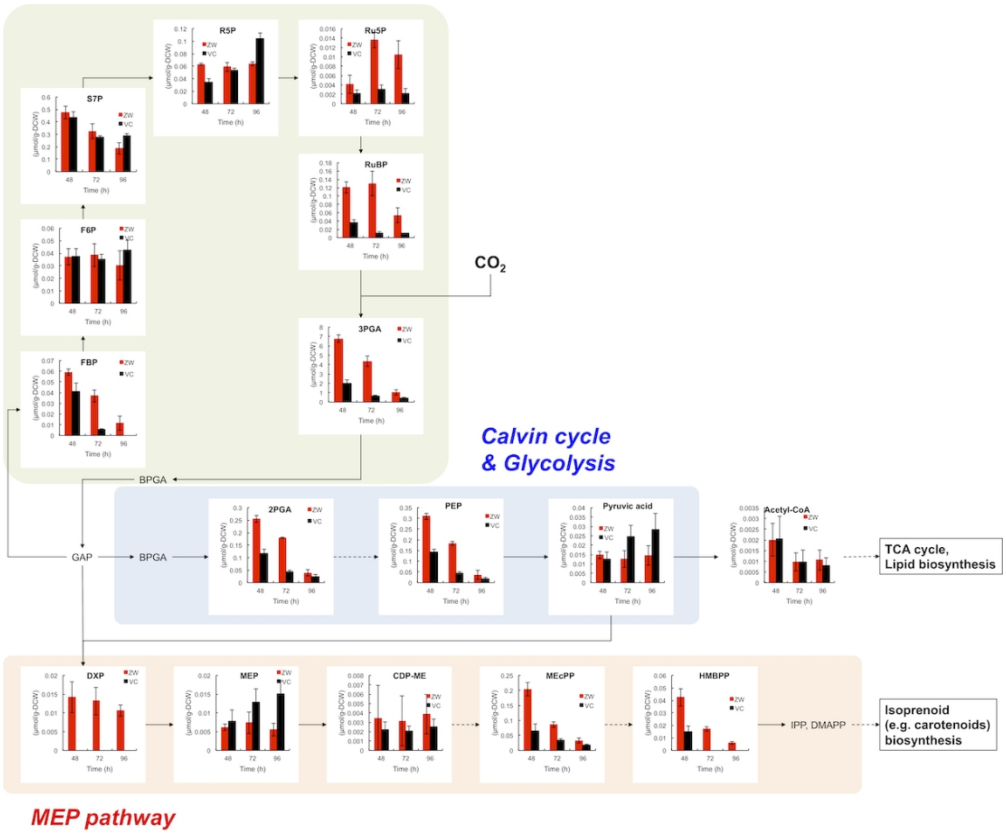

Figure 6

105x87mm (300 x 300 DPI)

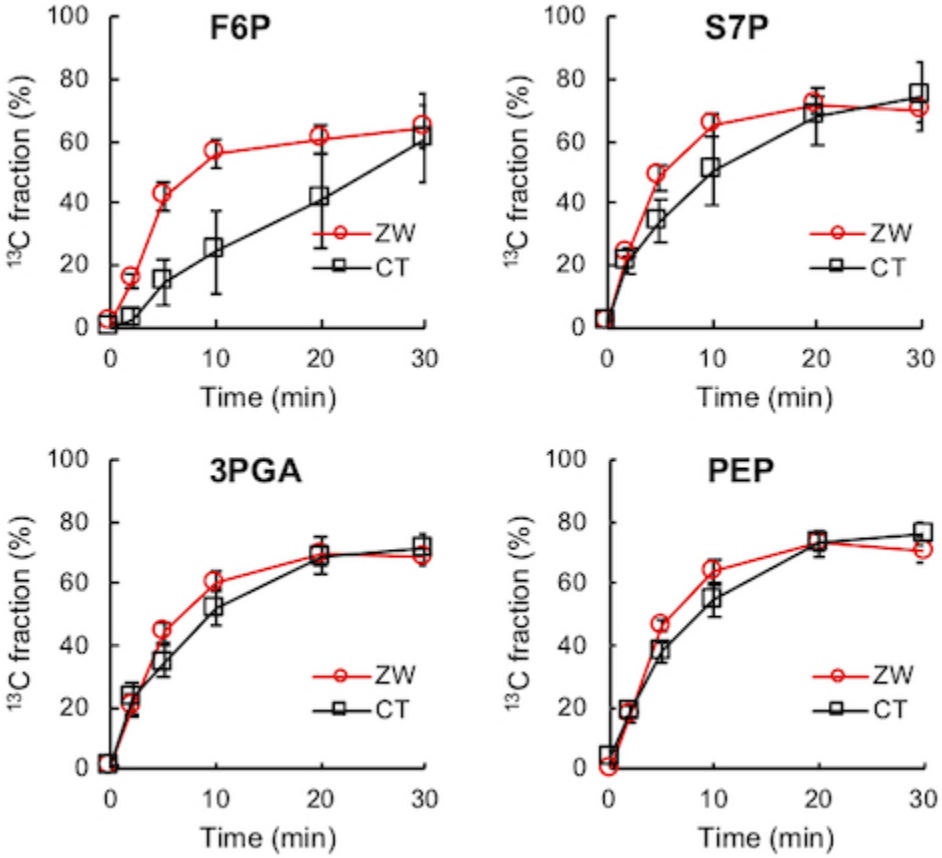

Figure 7

84x76mm (150 x 150 DPI)

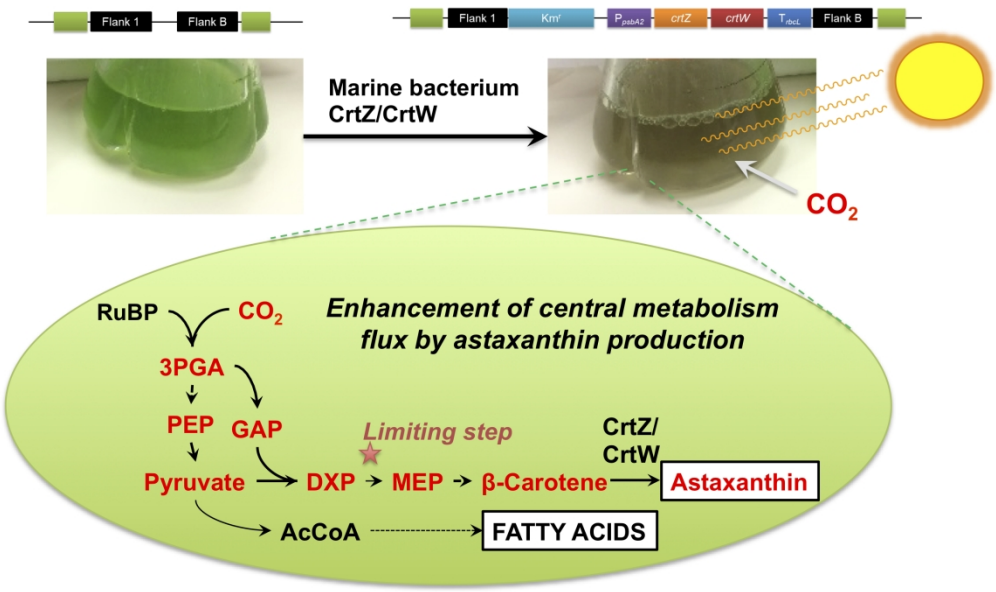

213x125mm (300 x 300 DPI)